Conference Proceedings
August 2015

OSAKA JAPAN

APCEAS
Asia-Pacific Conference on
Engineering & Applied Sciences

ACCMES
Asian Conference on
Civil, Material and Environmental Sciences

ACLSE
Annual Conference on
Life Sciences and Engineering

Conference Proceedings

25-27 August, 2015
Osaka, Japan

APCEAS

Asia-Pacific Conference on Engineering and Applied Science

ACCMES

Asian Conference on Civil, Material and Environmental Sciences

ACLSE

Annual Conference on Life Sciences and Engineering

APCEAS
Asia-Pacific Conference on Engineering and Applied Science
ISBN 978-986-90827-1-6

ACCMES
Asian Conference on Civil, Material and Environmental Sciences
ISBN 978-986-89298-0-7

ACLSE
Annual Conference on Life Sciences and Engineering
ISBN 978-986-90827-2-3

Conference Organization

APCEAS International Committee Board

Linda Osman-Schlegel, Deakin University (Geelong Waterfront Campus)

Khalid M. Mosalam, University of California, Berkeley

Chueerat Jaruskulchai, Kasetsart University

M. Cheralathan, SRM University

J N Bandyopadhyay, Indian Institute of Technology Kharagpur

S. Dhar, University of Calcutta

Poongothai Shankar, Annamalai University

Amit Agrawal, Indian Institute of Technology Bombay

Cheng Li, The Hong Kong Polytechnic University

T.M. Indra Mahlia, University of Malaya

Kunal Ghosh, Indian Institute of Technology Kanpur

Narayanan Kulathuramaiyer, University of Sarawak Malaysia

Arup K. Sarma, Indian Institute of Technology Guwahati

Suresh K Bhargava, School of Applied Sciences

Banerji P, Indian Institute of Technology Kharagpur

P.K. Ghosh, Indian Institute of Technology Poorkee

E George Dharma Prakash Raj, Bharathidasan University

R.P.Bhatnagar, Birla Institute of Technology

V. Vijayagopal, Annamalai University

Amit Awekar, Indian Institute of Technology Guwahati

Gustavo Carneiro, University of Adelaide

Pui-In Mak, University of Macau

E. Rathakrishnan, Indian Institute of Technology Kanpur

Bassim H. Hameed, University of Science Malaysia

Sudhirkumar Barai, Indian Institute of Technology Kharagpur

S. N. Sarkar, Calcutta University

Samit Bhattacharya, Indian Institute of Technology Kanpur

A. P. Shashikala, Birla Institute of Technology

RM. Senthamarai, Annamalai University

Arnab Bhattacharya, Indian Institute of Technology Kanpur

Zbigniew Michalewicz, University of Adelaide

B. Bhattacharya, Indian Institute of Technology Kharagpur

Amin Heidarpour, Monash University

Faizal Mustapha, Universiti Putra Malaysia

Susanta Banerjee, Indian Institute of Technology Kharagpur

M.V.L.R Anjaneyalu, Birla Institute of Technology

P. Balasubramanian, Universiti Teknologi PETRONAS

Hui Tong Chua, University of Western Australia

Andrew Whyte, Curtin University

Johnson Agbinya, La Trobe University

Yuen Ka Veng, University of Macau

ShahNor Basri, Universiti Putra Malaysia

T. V. Gopal, SRM University

Surendra Kumar, Indian Institute of Technology Poorkee

K. K. Saju, Cochin University of Science and Technology

Ghim Wei Ho, National University of Singapore

ACCMES International Committee Board

Abhijeet K. Digalwar, Birla Institute of Technology and Science

Alan K. T. Lau, The Hong Kong Polytechnic University

Aminaton Marto, Universiti Teknologi Malaysia

Ben Young, The University of Hong Kong

C.C. Sorrell, University of New South Wales

Cek Fauziah Ishak, Universiti Putra Malaysia

Chacko Jacob, Materials Science Centre

Choi Jaisung, Yonsei University

Gianluca Ranzi, The University of Sydney

Hannah Wan-Huan Zhou, University of Macau

Kartini Kamaruddin, Universiti Teknologi Mara

Jingsheng Chen, National University of Singapore

Jaisung Choi, University of Seoul

K.W. Chau, The Hong Kong Polytechnic University

Kanit Wattanavichien, Chulalongkorn University

L.N.Pattanaik, Birla Institute of Technology

M. Anusuyadevi Jayachandran, Bharathidhasan University

Manoj S Soni, The Birla Institute of Technology & Science

Mohd Razman Salim, Universiti Teknologi Malaysia

Monica Sharma, Malaviya National Institute of Technology Jaipur

Nasser Khalili, University of New South Wales

Nilanchal Patel, Birla Institute of Technology Mesra

Nilanjana Das, University of Calcutta

Norhayati Ahmad, MIMMM,CSci, Universiti Teknologi Malaysia

P.Sivaprakash, Karpagam Institute of Technology

Pramod Kumar Jain, Indian Institute of Technology Roorkee

PremRajP, National Institute of Technology Calicut

Renu Pawels, Cochin University of Science & Technology

S.Chandrakaran, National Institute of Technology Karnataka

Saxena, Ashok K, Indian Institute of Technology

Sharad Chandra Srivastava, B.I.T Mesra, Ranchi (Jharkhand)

Siti Mariyam Shamsuddin, Universiti Teknologi Malaysia

Sri Bandyopadhyay, University of New South Wales

Tuty Asma Abu Bakar, Universiti Teknologi Malaysia

V K Tewari, Indian Institute of Technology Kharagpur

Wiboonluk Pungrasmi, Chulalongkorn University

William K. Mohanty, Indian Institute of Technology

ACLSE International Committee Board

Asif Mahmood, King Saud University, Riyadh
Yung-Chih Kuo, Natinoal Chung Cheng University
Kyung-Suk Cho, Ewha Womans University
G.D.Ransinchung, Indian institute of Technology Roorkee
Shigeo Honma, Tokay University
Hasmawi Bin Khalid, University Teknologi Mara
Frank F.S. Shieu, National Chung Hsing University
Pakamas Chetpattananondh, Prince of Songkla University
Yung-Chih Kuo, Natinoal Chung Cheng University

APCEAS-199
Computational Simulations on Vibration Control of a Flexible Two-Link Manipulator by Piezoelectric Actuators Using Finite-Element Method

Abdul Kadir Muhammad
Ehime University
y861008b@mails.cc.ehime-u.ac.jp

Shingo Okamoto
Ehime University
okamoto.shingo.mh@ehime-u.ac.jp

Jae Hoon Lee
Ehime University
kadir_muhammad@yahoo.co.id

Abstract

The purposes of this research are to derive the equations of motion of a flexible two-link system by a finite-element method, to develop computational codes in order to perform dynamics simulations with vibration control and to propose an effective control scheme of a flexible two-link manipulator. The flexible two-link manipulator used in this paper consists of two aluminum beams as flexible links, two clamp-parts, two servo motors to rotate the links and two piezoelectric actuators to control vibration. Computational codes on time history responses, FFT (Fast Fourier Transform) processing and eigenvalues - eigenvectors analysis were developed to calculate the dynamic behavior of the links. Furthermore, a control scheme using the piezoelectric actuators was designed to suppress the vibration. Two proportional-derivative (PD) controllers were designed and demonstrated their performances. The calculated results of the controlled two-link manipulator revealed that the vibration of the flexible manipulator can be controlled effectively.

Keywords: Finite-element method, flexible manipulator, piezoelectric actuator, vibration control.

1. Introduction

Employment of flexible manipulators is recommended in the space and industrial applications in order to accomplish high performance requirements such as high-speed besides safe operation, increasing of positioning accuracy, and lower energy consumption, namely less weight. However, it is not usually easy to control a flexible manipulator because

of its inheriting flexibility. Deformation of the flexible manipulator when it is operated must be considered by any control. Its controller system should be dealt with not only its motion but also vibration due to the flexibility of the link.

The purposes of this research are to derive the equations of motion of a flexible two-link system by a finite-element method, to develop computational codes in order to perform dynamics simulations with vibration control and to propose an effective control scheme of a flexible two-link manipulator. The flexible two-link manipulator used in this paper consists of two aluminum beams as flexible links, two aluminum clamp-parts, two servo motors to rotate the links and two piezoelectric actuators to control vibration. Computational codes on time history responses, FFT (Fast Fourier Transform) processing and eigenvalues - eigenvectors analysis were developed to calculate the dynamic behavior of the links. Finally, two proportional-derivative controllers were designed to suppress the vibration. It was done by adding bending moments generated by the piezoelectric actuators to the two-link system.

2. Formulation by Finite-Element Method

The links have been discretized by finite-elements. Every finite-element (Element i) has two nodes namely Node i and Node (i+1). Every node (Node i) has two degrees of freedom [1] - [5], namely the lateral deformation $v_i(x,t)$, and the rotational angle $\psi_i(x,t)$. The length, the cross-sectional area and the area moment of inertia around z-axis of every element are denoted by l_i, S_i and I_{zi} respectively. Mechanical properties of every element are denoted as Young's modulus E_i and mass density ρ_i.

2.1 Kinematics

Figure 1 shows the position vectors r_{p1} and r_{p2} of arbitrary points P_1 and P_2 on Link 1 and Link 2 in the global and rotating coordinate frames. Let the links as flexible beams have a

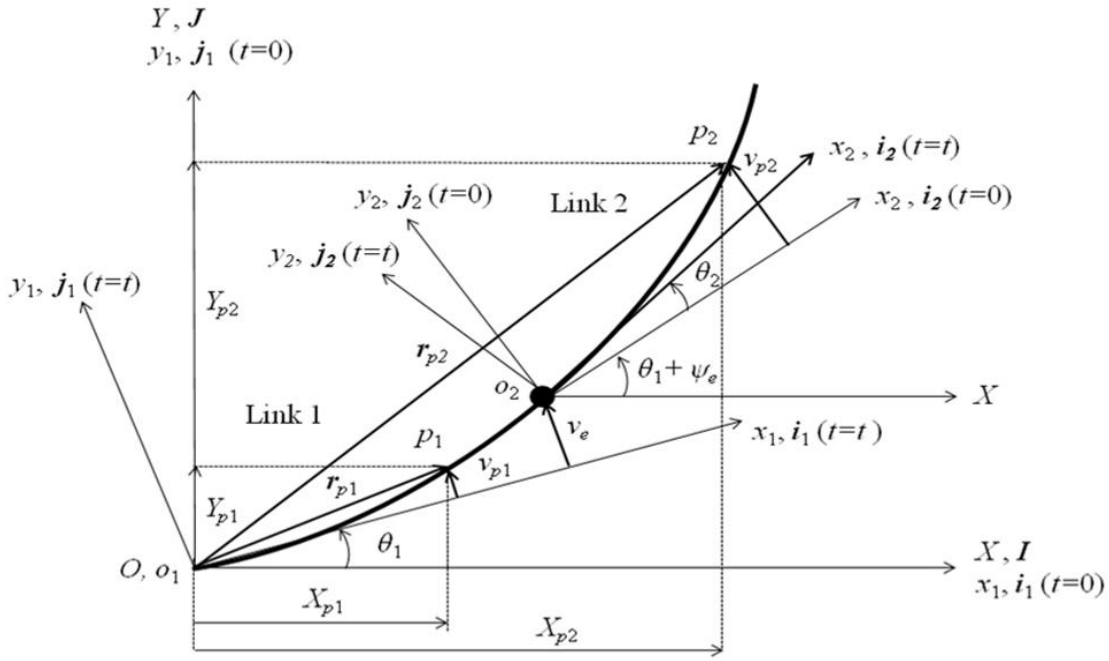

O-XY : Global coordinate frame

o_1-x_1y_1 : Rotating coordinate frame fixed to Link 1

o_2-x_2y_2 : Rotating coordinate frame fixed to Link 2

$r_{p1,}$ r_{p2} : Position vectors of the arbitrary points p_1 and p_2 in the X-axis of the O-XY

θ_1 : Rotational angle of the first motor

θ_2 : Rotational angle of the second motor

$X_{p1,}$ X_{p2} : Coordinates of the arbitrary points p_1 and p_2 in the X-axis of the O-XY

Y_{p1}, Y_{p2} : Coordinates of the arbitrary points p_1 and p_2 in the Y-axis of the O-XY

v_{p1} : Lateral deformation of the arbitrary point p_1 on Link 1 in the o_1-x_1y_1

v_{p2} : Lateral deformation of the arbitrary point p_2 on Link 2 in the o_2-x_2y_2

ψ_e : Rotational angle of the end-point of Link 1

v_e : Lateral deformation of the end-point of Link 1

L_1 : Length of Link 1

Fig. 1: Position vectors of arbitrary points P_1 and P_2 in the global and

motion that is confined in the horizontal plane as shown in Fig. 1. The $O - XY$ frame is the global coordinate frame with Z-axis is fixed. Furthermore, $o_1 - x_1y_1$ and $o_2 - x_2y_2$ are the rotating coordinate frames fixed to the root of Link 1 and Link 2, respectively (z_1-axis and z_2-axis are fixed). The unit vectors in X, Y, x_1, y_1, x_2 and y_2 axes are denoted by I, J, i_1, j_1, i_2 and j_2, respectively. The first motor is installed on the root of Link 1. The second motor that treated as a concentrated mass is installed in the root of Link 2. The rotational angles of the first and second motor when the links rotate are denoted by $\theta_1(t)$ and $\theta_2(t)$. Length of Link 1 is donated by L_1. Lateral deformation of the arbitrary points P_1 and P_2 in the first and the second links are donated by v_{p1} and v_{p2}, respectively. Lateral deformation and rotational angel

of the end-point of the first link are donated by v_e and ψ_e, respectively. The position vectors r_{p1} and r_{p2} of the arbitrary points P_1 and P_2 at time $t = t$, measured in the $O - XY$ frame shown in Fig. 1 are expressed by

$$\boldsymbol{r}_{p1} = X_{p1}(x_1, \theta_1, v_{p1}, t)\boldsymbol{I} + Y_{p1}(x_1, \theta_1, v_{p1}, t)\boldsymbol{J} \quad (1)$$

$$\boldsymbol{r}_{p2} = X_{p2}(x_2, \theta_1, \theta_2, v_e, \psi_e, v_{p2}, t)\boldsymbol{I} + Y_{p2}(x_2, \theta_1, \theta_2, v_e, \psi_e, v_{p2}, t)\boldsymbol{J} \quad (2)$$

In this research, there are four boundary conditions together at nodes i and (i+1) when the one-dimensional and two-node element is used. The four boundary conditions are expressed as nodal vector as follow [6]

$$\boldsymbol{\delta}_i = \{v_i \quad \psi_i \quad v_{i+1} \quad \psi_{i+1}\}^T \quad (3)$$

Then, the relation between the lateral deformation v_i, the rotational angle ψ_i and the strain ε_i of Node i can be found in [1] - [5].

2.2 Equations of Motion

Equations of motion of Element i on Link 1 and Link 2 are respectively given by

$$\boldsymbol{M}_i\ddot{\boldsymbol{\delta}}_i + \boldsymbol{C}_i\dot{\boldsymbol{\delta}}_i + \left[\boldsymbol{K}_i - \dot{\theta}_1^{\,2}\boldsymbol{M}_i\right]\boldsymbol{\delta}_i = \ddot{\theta}_1\boldsymbol{f}_i \quad (4)$$

$$\boldsymbol{M}_i\ddot{\boldsymbol{\delta}}_i + \boldsymbol{C}_i\dot{\boldsymbol{\delta}}_i + \left[\boldsymbol{K}_i - \left(\dot{\theta}_1 + \dot{\psi}_e + \dot{\theta}_2\right)^2\boldsymbol{M}_i\right]\boldsymbol{\delta}_i = \left(\ddot{\theta}_1 + \ddot{\psi}_e + \ddot{\theta}_2\right)\boldsymbol{f}_i + \left(L_1\ddot{\theta}_1 + \ddot{v}_e - v_e\dot{\theta}_1^{\,2}\right)\cos(\psi_e + \theta_2)\boldsymbol{g}_i$$
$$+\left(v_e\ddot{\theta}_1 + L_1\dot{\theta}_1^{\,2} + \frac{1}{2}\dot{v}_e\left(3\dot{\theta}_1 - \dot{\psi}_e - \dot{\theta}_2\right)\right)\sin(\psi_e + \theta_2)\boldsymbol{g}_i \quad (5)$$

where M_i, C_i, and K_i, are the mass matrix, damping matrix, stiffness matrix of Element i on Link 1 and Link 2. Vectors of f_i and g_i are the excitation vectors on Link 1 and Link 2. The representation of the matrices and the vector of f_i can be found in [1] and [3]. The vector of g_i can be defined by

$$\boldsymbol{g}_i = \frac{\rho_i S_i l_i}{12}\{-6 \quad 15l_i \quad 6 \quad l_i\}^T \quad (6)$$

Finally, the equations of motion of Link 1 and Link 2 with n elements considering the boundary conditions is given by

$$\boldsymbol{M}_n\ddot{\boldsymbol{\delta}}_n + \boldsymbol{C}_n\dot{\boldsymbol{\delta}}_n + \left[\boldsymbol{K}_n - \dot{\theta}_1^{\,2}\boldsymbol{M}_n\right]\boldsymbol{\delta}_n = \ddot{\theta}_1\boldsymbol{f}_n \quad (7)$$

$$\boldsymbol{M}_n\ddot{\boldsymbol{\delta}}_n+\boldsymbol{C}_n\dot{\boldsymbol{\delta}}_n+\left[\boldsymbol{K}_n-\left(\dot{\theta}_1+\dot{\psi}_e+\dot{\theta}_2\right)^2\boldsymbol{M}_n\right]\boldsymbol{\delta}_n=\left(\ddot{\theta}_1+\ddot{\psi}_e+\ddot{\theta}_2\right)\boldsymbol{f}_n+\left(L_1\ddot{\theta}_1+\ddot{v}_e-v_e\dot{\theta}_1^2\right)\cos(\psi_e+\theta_2)\boldsymbol{g}_n$$
$$+\left(v_e\ddot{\theta}_1+L_1\dot{\theta}_1^2+\frac{1}{2}\dot{v}_e\left(3\dot{\theta}_1-\dot{\psi}_e-\dot{\theta}_2\right)\right)\sin(\psi_e+\theta_2)\boldsymbol{g}_n \qquad (8)$$

3. Validation of the Formulation

3.1 Experimental Model

Figure 3 shows the experimental model of the flexible two-link manipulator. The flexible manipulator consists of two flexible aluminum beams, two clamp-parts, two servo motors and the base. Link 1 and Link 2 are attached to the first and second motors through the clamp-parts. Link 1 and Link 2 are connected through the second motor. Two strain gages are bonded to the position of 0.11 [m] and 0.38 [m] from the origin of the two-link system. The first motor is mounted to the base. In the experiments, the motors were operated by an independent motion controller.

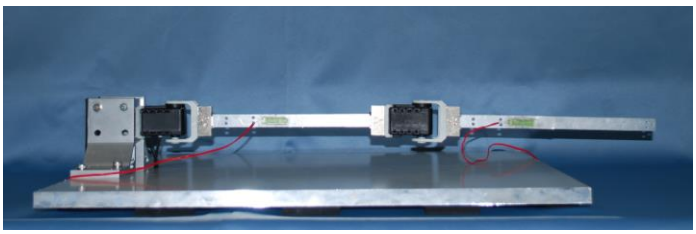

Fig. 3: Experimental model of the flexible two-link manipulator

3.2 Computational Models

In this research, we defined and used three types of computational models of the flexible two-link manipulator.

3.2.1 Model Ⅰ

A model of only a two-link manipulator was used as Model Ⅰ. Figure 5.a shows Model Ⅰ. The links and the clamp-parts were discretized by 35 elements. Two strain gages are bonded to the position of Node 6 and Node 22 of the two-link (0.11 [m] and 0.38 [m] from the origin), respectively.

3.2.2Model Ⅱ

A model of the flexible two-link manipulator including one piezoelectric actuator was defined as Model Ⅱ. Figure 5.b shows model Ⅱ. The piezoelectric actuator was bonded to the one surface of Element 4. The links including the clamp-parts and the piezoelectric actuator were discretized by 36 elements.

The piezoelectric actuator suppresses the vibration of the two-link flexible manipulator by adding bending moments at Nodes 3 and 6 of the two-link manipulator, M_3 and M_6. The bending moments are generated by applying voltages E_1 to the piezoelectric actuator. The bending moments proportional to the voltage which are expressed by

$$M_3 = -M_6 = d_{11}E_1 \tag{9}$$

Here d_{11} is a constant quantity and M_3 opposites to M_6.

Furthermore, the voltage to generate the bending moments is proportional to the strains ε_1 of the two-link due to the vibration. The relations can be expressed as follows

$$E_1 = \pm\frac{1}{d_{21}}\varepsilon_1 \tag{10}$$

Here d_{21} is a constant quantity.

3.2.3 Model Ⅲ

A model of the flexible two-link manipulator including two piezoelectric actuators was defined as Model Ⅲ. Figure 5.c shows Model Ⅲ. The piezoelectric actuators were bonded to the one surface of Elements 4 and 20. The links including the clamp-parts and the piezoelectric actuators were discretized by 36 elements. Schematic representations on modeling of the piezoelectric actuators are shown in Fig. 4. Physical parameters of the flexible two-link manipulator model and the piezoelectric actuators are shown in table 1.

The first piezoelectric actuator suppresses the vibration of the two-link flexible manipulator by adding bending moments at Nodes 3 and 6 of the two-link manipulator, M_3 and M_6. The second piezoelectric actuator suppresses the vibration of the two-link flexible manipulator by adding bending moments at nodes 19 and 22 of the two-link manipulator, M_{19} and M_{22}. The bending moments are generated by applying voltages E_1 and E_2 to the actuators.

Table 1: Physical parameters of the flexible two-link and the piezoelectric actuators

l : Total length	m	4.05×10^{-1}
l_1 : Length of Link 1	m	1.90×10^{-1}
l_2 : Length of Link 2	m	2.15×10^{-1}
l_{c1}, l_{c2} : Length of clamp-parts 1 and 2	m	1.50×10^{-2}
l_{a1}, l_{a2} : Length of Actuators 1 and 2	m	2.00×10^{-2}
S_{l1}, S_{l2} : Cross section area of links 1 and 2	m^2	1.95×10^{-5}
S_{c1}, S_{c2} : Cross section area of clamp-parts 1 and 2	m^2	8.09×10^{-4}
S_{a1}, S_{a2} : Cross section area of actuators 1 and 2	m^2	1.58×10^{-5}
I_{zl1}, I_{zl2} : Cross section area moment of inertia around z-axis of links 1 and 2	m^4	2.75×10^{-12}
I_{zc1}, I_{zc2} : Cross section area moment of inertia around z-axis of clamp-parts 1 and 2	m^4	3.06×10^{-8}
I_{za1}, I_{za2} : Cross section area moment of inertia around z-axis of actuators 1 and 2	m^4	1.61×10^{-11}
E_{l1}, E_{l2} : Young's Modulus of links 1 and 2	GPa	7.03×10^{1}
E_{c1}, E_{c2} : Young's Modulus of clamp-parts 1 and 2	GPa	7.03×10^{1}
E_{a1}, E_{a2} : Young's Modulus of actuators 1 and 2	GPa	4.40×10^{1}
ρ_{l1}, ρ_{l2} : Density of links 1 and 2	kg/m^3	2.68×10^{3}
ρ_{c1}, ρ_{c2} : Density of clamp-parts 1 and 2	kg/m^3	2.68×10^{3}
ρ_{a1}, ρ_{a2} : Density of actuators 1 and 2	kg/m^3	3.33×10^{3}
α_1, α_2 : Damping factors of links 1 and 2	s	2.50×10^{-4}
E_1, E_2 : Maximum input voltages of actuators 1 and 2	V	150.00
F_1, F_2 : Maximum output forces of actuators 1 and 2	N	200.00
m_2 : Mass of the second motor and it's clamping system	g	113.53

The bending moments proportional to the voltages which are expressed by Eq. (9) and

$$M_{19} = -M_{22} = d_{12} E_2 \tag{11}$$

Here d_{12} is a constant quantity and M_{19} opposites to M_{22}.

Furthermore, the voltages to generate the bending moments are proportional to the strains ε_1 and ε_2 of the two-link due to the vibration. The relations can be expressed by Eq. (10) and

$$E_2 = \pm \frac{1}{d_{22}} \varepsilon_2 \tag{12}$$

Here d_{22} is a constant quantity. Then, d_{11}, d_{12}, d_{21} and d_{22} will be determined by comparing the calculated results and experimental ones.

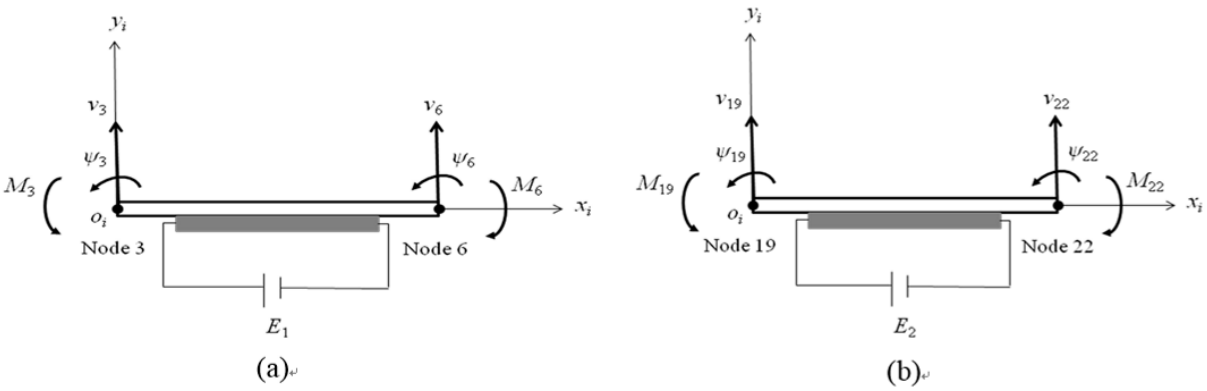

Fig. 4: Modeling of piezoelectric actuators: (a) Modeling of Actuator 1, (b) Modeling of Actuator 2

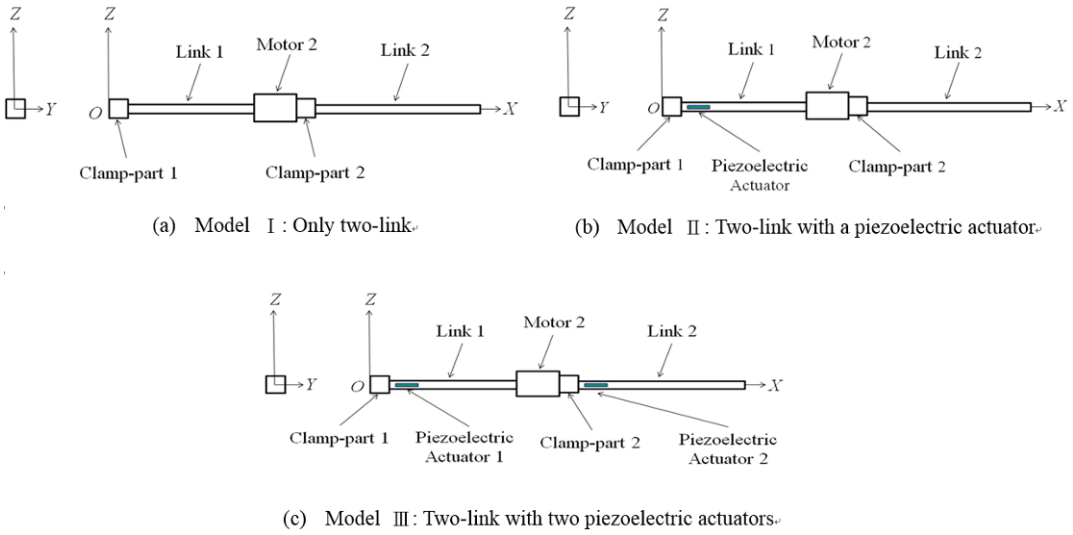

Fig. 5: Computational models of the flexible two-link manipulator

3.3 Time History Responses of Free Vibration

Experiment on free vibration was conducted using an impulse force as an external one. Figure 6.a shows the experimental time history response of strains, ε_e on the free vibration at the same position in the calculation (0.11 [m] from the origin of the two-link system). Furthermore, the computational codes on time history response of Model Ⅰ were developed. Figure 6.b shows the calculated strains at Node 6 of Model Ⅰ under the impulse force.

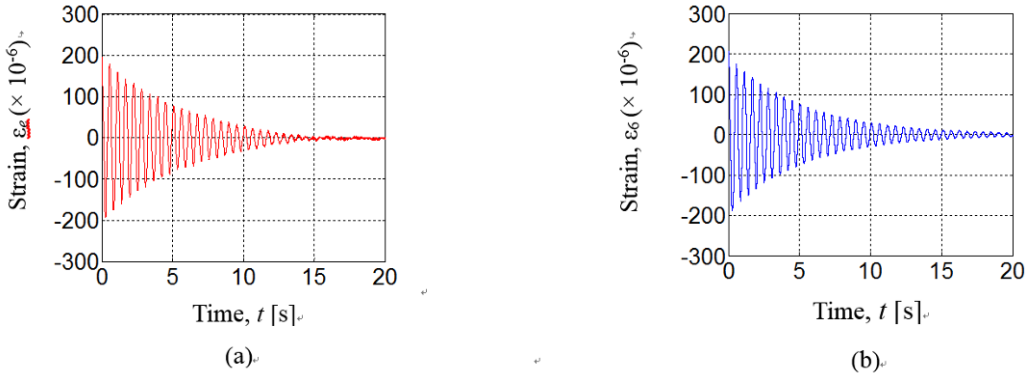

Fig. 6: Time history responses of strains on free vibration: (a) Experimental strains at 0.11 [m] from the origin of the two-link, (b) Calculated strains at Node 6 of Model Ⅰ

3.4.4 FFT (Fast Fourier Transform) Processing

Both the experimental and calculated time history responses of strains on free vibration were transferred by FFT processing to find their frequencies. Figures 7.a and 7.b show the experimental and calculated natural frequencies of the flexible two-link manipulator, respectively. The first experimental natural frequency, 1.79 Hz agreed with the calculated one, 1.80 Hz. The second experimental natural frequency could not be measured. However, in the calculation, it could be obtained as 8.95 Hz.

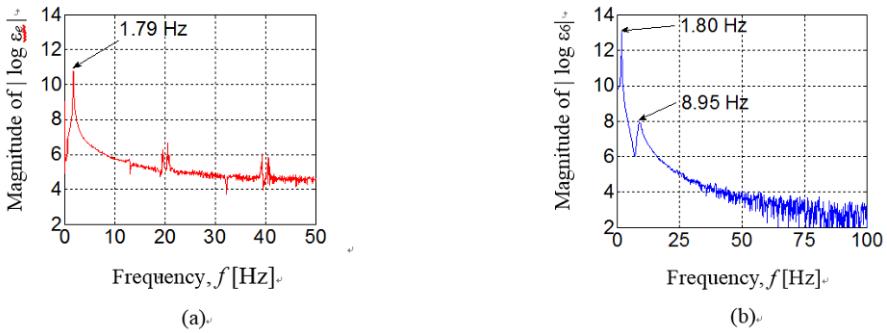

Fig. 7: Natural frequencies: (a) Experimental natural frequency of the flexible two-link, (b) Calculated natural frequencies of Model Ⅰ

3.5 Eigen-values and Eigen-vectors Analysis

The computational codes on Eigen-values and Eigen-vectors analysis were developed for natural frequencies and vibration modes. The calculated results for the first and second natural frequencies were 1.79 Hz and 8.92 Hz, respectively. The vibration modes of natural frequencies are shown in Fig. 8.

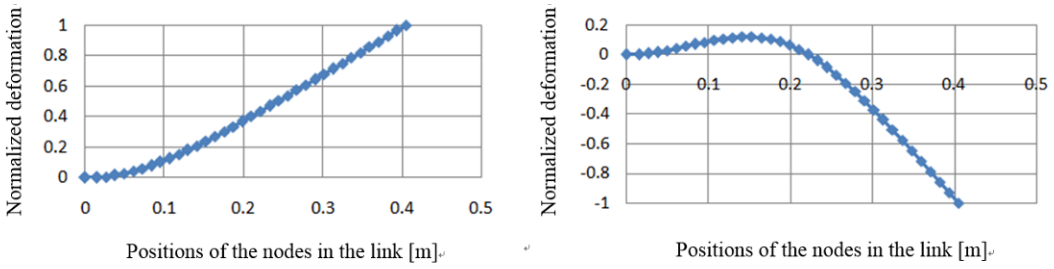

(a) First vibration mode and natural frequency ($f_1 = 1.79$ Hz) (b) Second vibration mode and natural frequency ($f_2 = 8.92$ Hz)

Fig. 8: Vibration modes and natural frequencies

3.6 Time History Responses Due to the Base Excitations

Another experiment was conducted to investigate the vibration of the flexible two-link due to the base excitations generated by rotation of the motors. In the experiment, the motors were rotated by the angle of $\pi/2$ radians (90 degrees) within 0.50 [s]. Figures 9.a and 10.a show the experimental time history responses of strains of the flexible two-link due to the motors' rotation at 0.11 [m] and 0.38 [m] from the origin of the link, respectively. Furthermore, based on Figures 9.a and 10.a, the time history response of strains at Node 6 and Node 22 of Model Ⅰ were calculated as shown in Figures 9.b and 10.b, respectively.

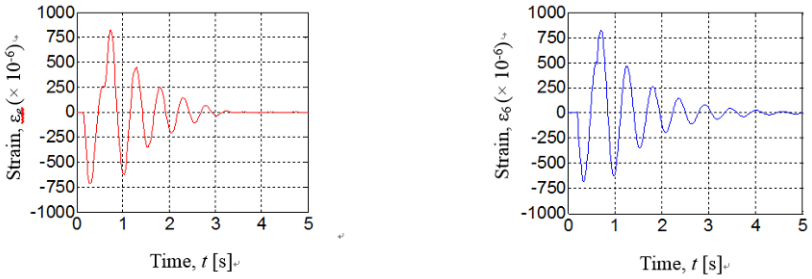

Fig. 9: Time history responses of strains due to base excitation: (a) Experimental strains at 0.11 [m] from the origin of the two-link, (b) Calculated strains at Node 6 of Model Ⅰ

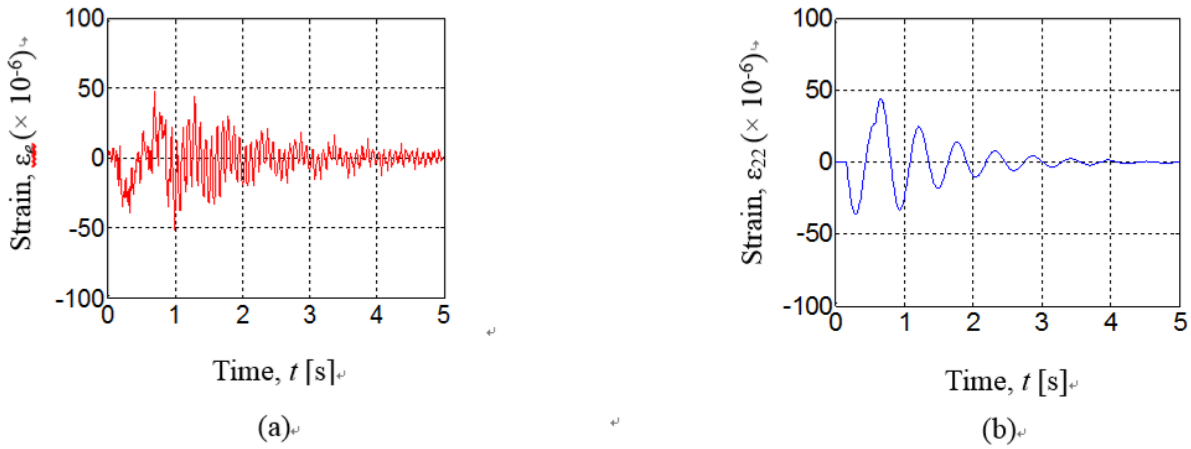

Fig. 10: Time history responses of strains due to base excitation: (a) Experimental strains at 0.38 [m] from the origin of the two-link, (b) Calculated strains at Node 22 of Model I

4. Control Scheme and Simulations

4.1 Control Scheme

A control scheme to suppress the vibration of the two-link system was designed using one and two piezoelectric actuators. It was done by adding bending moments generated by the piezoelectric actuators to the two-link system. To drive the actuators, two proportional-derivative (PD) controllers have been designed and examined.

4.1.1 Using a Piezoelectric Actuator

The piezoelectric actuator suppresses the vibration of the two-link flexible manipulator by adding bending moments at nodes 3 and 6 of the two-link manipulator, M_3 and M_6. Therefore, the equation of motion of Link 1 become

$$\boldsymbol{M}_n\ddot{\boldsymbol{\delta}}_n + \boldsymbol{C}_n\dot{\boldsymbol{\delta}}_n + \left[\boldsymbol{K}_n - \dot{\theta}_1^{\,2}\boldsymbol{M}_n\right]\boldsymbol{\delta}_n = \ddot{\theta}_1\boldsymbol{f}_n + \boldsymbol{u}_{1n} \tag{13}$$

where the vector of u_{1n} containing M_3 and M_6 is the control force generated by the actuator to the two-link system.

Based on Eq. (9) and Eq. (10) the bending moments can be defined in term of the PD-controller as follows

$$M_3 = -M_6 = \left(K_p + K_d\, s\right)\left(\varepsilon_d(s) - \varepsilon_6(s)\right) \tag{14}$$

where ε_d and ε_6 denote the desired and measured strains at Node 6, respectively.

A block diagram of the PD-controller for the two-link system using one actuator is shown in Fig. 11.

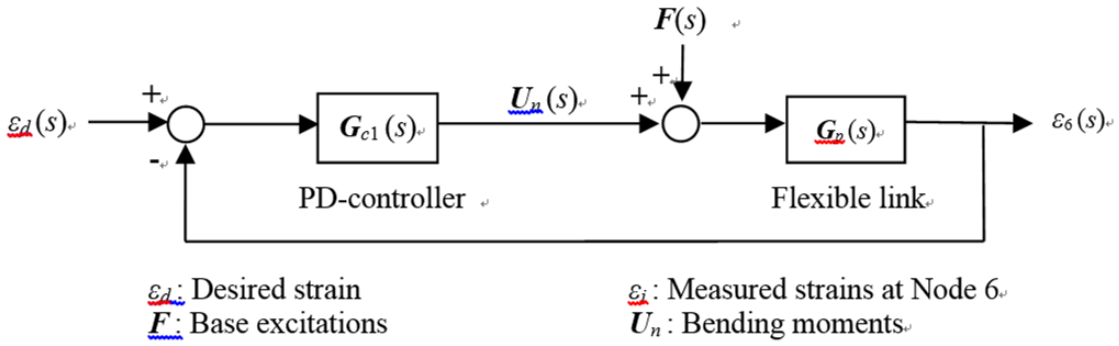

Fig. 11: Block diagram of PD-controller of the flexible two-link manipulator using a

4.1.2 Using Two Piezoelectric Actuators

The first piezoelectric actuator suppresses the vibration of the two-link flexible manipulator by adding bending moments at Nodes 3 and 6 of the two-link manipulator, M_3 and M_6, as explained in sub-chapter 4.1.1. The second piezoelectric actuator suppresses the vibration of the two-link flexible manipulator by adding bending moments at Nodes 19 and 22 of the two-link manipulator, M_{19} and M_{22}. Therefore, the equation of motion of Link 1 is shown in Eq. (13) and the equation of motion of Link 2 in given by

$$\boldsymbol{M}_n\ddot{\boldsymbol{\delta}}_n + \boldsymbol{C}_n\dot{\boldsymbol{\delta}}_n + \left[\boldsymbol{K}_n - \left(\dot{\theta}_1 + \dot{\psi}_e + \dot{\theta}_2\right)^2 \boldsymbol{M}_n\right]\boldsymbol{\delta}_n = \left(\ddot{\theta}_1 + \ddot{\psi}_e + \ddot{\theta}_2\right)\boldsymbol{f}_n + \left(L_1\ddot{\theta}_1 + \ddot{v}_e - v_e\dot{\theta}_1^{\,2}\right)\cos(\psi_e + \theta_2)\boldsymbol{g}_n$$
$$+\left(v_e\ddot{\theta}_1 + L_1\dot{\theta}_1^{\,2} + \frac{1}{2}\dot{v}_e\left(3\dot{\theta}_1 - \dot{\psi}_e - \dot{\theta}_2\right)\right)\sin(\psi_e + \theta_2)\boldsymbol{g}_n + \boldsymbol{u}_{2n} \tag{15}$$

where the vector of u_{2n} containing M_{19} and M_{22} is the second control force generated by the second piezoelectric actuator to the two-link system.

Based on Equations (9), (10), (11) and (12) the bending moments can be defined in term of the first and second PD-controllers as follows

$$M_3 = -M_6 = \left(K_{p1} + K_{d1}\,s\right)\left(\varepsilon_d(s) - \varepsilon_6(s)\right) \tag{16}$$

$$M_{19} = -M_{22} = \left(K_{p2} + K_{d2}\,s\right)\left(\varepsilon_d(s) - \varepsilon_{22}(s)\right) \tag{17}$$

where ε_d, ε_6 and ε_{22} denote the desired and measured strains at Node 6 and Node 22, respectively.

A block diagram of the PD-controls for the two-link system using two actuators is shown in Fig. 12.

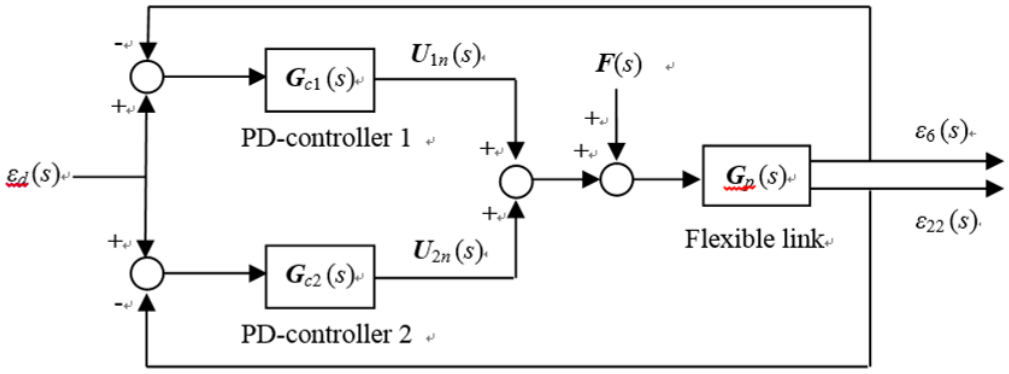

ε_d : Desired strain
F : Base excitations
ε_6 and ε_{22} : Measured strains at Nodes 6 and 22
U_{1n} and U_{2n} : Bending moments generated by actuators 1 and 2

Fig. 12: Block diagram of PD-controllers of the flexible two-link manipulator using two piezoelectric actuators

4.2 Calculated Results

Time history responses of strains at Node 6 and Node 22 on the uncontrolled and controlled system were calculated for Models Ⅱ and Ⅲ when the first and second motors rotated $\pi/4$ radians (45 degrees) and $\pi/2$ radians (90 degrees) within 0.50 [s], respectively. Time history responses of strains on the controlled system for Models Ⅱ and Ⅲ were calculated under control scheme shown in Figures 13 and 14, respectively.

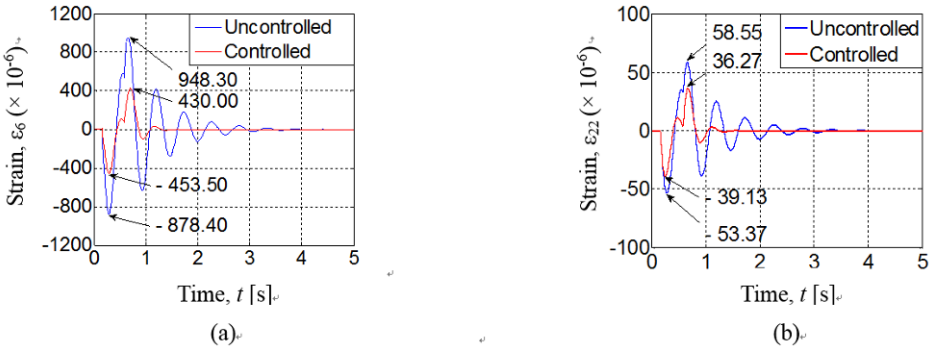

Fig. 13: Calculated time history responses of strains for uncontrolled and controlled Model Ⅱ due to the base excitations: (a) at Node 6, (b) at Node 22

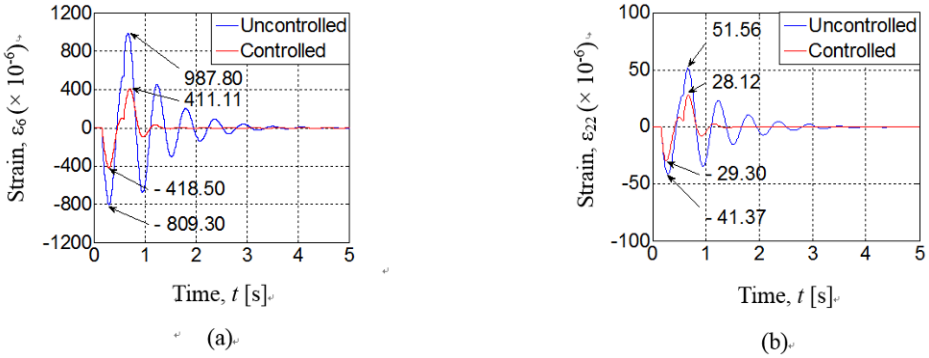

Fig. 14: Calculated time history responses of strains for uncontrolled and controlled Model Ⅲ due to the base excitations: (a) at Node 6, (b) at Node 22

Examining several gains of the PD-controller using one actuator leaded to K_p = 2 [Nm] and K_d = 0.6 [Nms] as the better ones. Furthermore, examining several gains of the PD- controllers using two actuators leaded to K_{p1} = 2 [Nm], K_{d1} = 0.6 [Nms], K_{p2} = 40 [Nm] and K_{d2} = 10 [Nms] as the better ones. The controller gains were examined considering the maximum output forces of the actuators. Figures 13 and 14 show the uncontrolled and controlled time history responses of strains for Models Ⅱ and Ⅲ, respectively. The maximum strains of uncontrolled system for Model Ⅱ at Node 6 and Node 22 were 948.30×10^{-6} and 58.55×10^{-6}, respectively. By using PD-controller they become 453.50×10^{-6} and 39.13×10^{-6}, respectively, as shown in Figures 13.a and 13.b. The maximum strains of uncontrolled system for Model Ⅲ at Node 6 and Node 22 were 987.80×10^{-6} and 51.56×10^{-6}, respectively. By using PD-controller they become 418.50×10^{-6} and 29.30×10^{-6}, respectively, as shown in Figures 14.a and 14.b.
It was verified from these results that the proposed control scheme can effectively suppress the vibration of the flexible two-link manipulator even though using only one piezoelectric actuator.

5. Conclusion

The equations of motion for the flexible two-link manipulator had been derived using the finite-element method. Computational codes had been developed in order to perform dynamics simulations of the system. Experimental and calculated results on time history responses, natural frequencies and vibration modes show the validities of the formulation, computational codes and modeling of the system. Two proportional-derivative controllers were designed to suppress the vibration of the system. The calculated results have been revealed that the vibration of the system can be suppressed effectively even though using only one piezoelectric actuator.

6. References

[1] A.K. Muhammad., S. Okamoto., & J.H. Lee. (2014). Computer simulations on vibration control of a flexible single-link manipulator using finite-element method. *Proceeding of 19th International Symposium of Artificial Life and Robotics*, 381 – 386.

[2] A.K. Muhammad., S. Okamoto., & J.H. Lee. (2014). Computer simulations and experiments on vibration control of a flexible link manipulator using a piezoelectric actuator. *Lecture Notes in Engineering and Computer Science: Proceeding of The International MultiConference of Engineers and Computer Scientists* 2014, 262 – 267.

[3] A.K. Muhammad., S. Okamoto., & J.H. Lee. (2014). Comparison of proportional-derivative and active-force controls on vibration of a flexible single-link manipulator using finite-element method. *Journal of Artificial Life and Robotics, 19(4)*, 375 – 381. doi: 10.1007/s10015-014-0186-5

[4] A.K. Muhammad., S. Okamoto., & J.H. Lee. (2014). Comparisons of proportional and active-force controls on vibration of a flexible link manipulator using a piezoelectric actuator through calculations and experiments. *Engineering Letters, 22(3)*, 134 – 141.

[5] A.K. Muhammad., S. Okamoto., & J.H. Lee. (2015). Active-force control on vibration of a flexible single-link manipulator using a piezoelectric actuator. In G.-C. Yang., S.-I. Ao., X. Huang., & O. Castilo (Eds.), *Transactions on Engineering Technologies, 2014,* (pp. 1 – 15). Springer. doi: 10.1007/978-94-017-9588-3_1

[6] M. Lalanne., P. Berthier., & J.D. Hagopian. (1983), *Mechanical Vibration for Engineers*, (pp. 146 – 153). John Wiley & Sons Ltd.